Int. J. New. Chem., 2021, Vol. 8, Issue 4, pp. 386-399.

International Journal of New Chemistry

Published online 2021 in http://www.ijnc.ir/.

Open Access

Print ISSN: 2645-7237

Online ISSN: 2383-188x

Original Research Article

Intrinsic distortion in the analysis of the Jahn-Teller effect: by Transition state theory (TST) and Nitrogen inversion

Golrokh Mahmoudzadeh*

Department of Chemistry, Arak Branch, Islamic Azad University, Arak, Iran

Received: 2020-10-22 *Accepted: 2021-06-30* *Published: 2021-10-01*

ABSTRACT

In the case of NH_3, two reasonable geometries can be tried. Molecular orbitals are the main electronic structural units for analysis and solution of chemical problems at the electronic level and Quantum mechanical description of the changes in electronic structure due to distortions in molecular shape and vice versa is given in the form of the vibronic coupling theory. The most famous concept based on this theory is the Jahn−Teller (JT) effect. The second-order Jahn-Teller effect (SOJT) is an example of reactions proceeding by an interaction between the HOMO and the LUMO within the same molecule In the high-symmetry regular triangular configuration D_{3h} with the N atom in the center, the ground-state configuration of the system is singlet $^1A_1'$, that in the direction coordinate instability of $Q_{a2"}$ with the time-dependent DFT (TD-DFT) calculations symmetry descents and to form a square-pyramidal structure. The intrinsic reaction coordinate (IRC) theory in the present paper is presented for further understanding of the mechanism of such distortion. Natural bond analysis (NBO) is used for illustrating the strongest interaction and natural atomic charges of these structures. The calculated energy profile has been supplemented with optimization by means of transition state theory (TST).

Keywords: Intrinsic Reaction Coordinate (IRC), Time-dependent DFT (TD-DFT), Normal Coordinate (*Q*), Natural bond analysis (NBO), Transition State Theory (TST).

***Corresponding Author: Tel.: +989143434088**
E-mail: gmahmoudzadeh@yahoo.com

Introduction

Intrinsic Reaction Coordinate (IRC) calculations can be used to check that the given transition state is the expected transition state for the reaction of interest. IRC calculations start at a transition state and move downhill in energy along the reaction path toward a minimum of the potential energy surface, calculating a series of points in which all geometric variables orthogonal to the path are optimized. The calculations can be run in the forward direction (toward the products) and the backward direction (toward the reactants). A transition state is a first - order saddle point on a potential energy surface (PES) [1]. The vibrational spectrum of a transition state is characterized by one imaginary frequency, implying a negative force constant. This means that in one direction in nuclear-configuration space, the energy has a maximum, while in all other (orthogonal) directions, the energy is a minimum. In order to verify if a stationary point is a transition state, a vibrational frequency calculation must be performed at the same computational level as for geometry optimization. The normal mode corresponding to the imaginary frequency in the transition state usually reflects the change in geometry in going from reactants to products. One more feature that can be very useful when examining transition states, the Internal Reaction Coordinate (IRC) is related to the minimum energy path (MEP), which is defined as the steepest descent path starting from the transition state, initially going in the direction of negative curvature in the Hessian. The path can be followed backwards (to reactants) and forward (to products). Following this path can indicate if you really found the transition state that connects the two minima of interest. The IRC is defined in terms of mass-weighted Cartesian coordinates and it has a well-defined step length. Computationally, once a transition state is found, it is possible to restart from the checkpoint file (name.chk) and perform and IRC [2].

Computational Details

All electronic structure calculations were carried out by means of the Gaussian 09 software package [3]. Molecular structures were visualized with Gauss View [4]. The molecular structures and vibrational frequencies of all stationary points were computed at the Hartree-Fock method. Hartree-Fock computations were carried out using the STO-3G basis set [5-7]. The nature of all optimized structures were determined according to the calculations of vibrational frequencies which were calculated at the same levels of theory to ensure that a minimum on the potential

energy surface was obtained under the imposed constraint of the indicated symmetry. Energy minima possess the Hessian matrix with no negative eigenvalues, whereas transition state has one and only one negative eigenvalue corresponds to the motion of the atoms over a first-order saddle point [8-9].

Time-dependent density functional theory (TD-DFT) [10], which is one of the most popular tools in the study of excited states of molecular systems, was used to study the electronic configurations of the planar and pyramidal structures of molecule NH_3. It should be noted that TD-DFT has become a powerful tool in predicting optical response properties of molecules. In the high-symmetry regular triangular configuration D_{3h} with the N atom in the center, the electronic configuration of the system is singlet $^1A_1'$, so that an excited state is required to have symmetry to produce the PJT effect. . The population analysis has also been performed by the natural bond orbital method [11] at Hartree-Fock level of theory using NBO 6.0 program [12] under Gaussian 2009 program package.

Results and discussion

Planar and Pyramidal Interconversions

The zero- point (ZPE) and total electronic (E_{el}) energies (E_o = Eel + ZPE) obtained from geometry optimization of the planar (D_{3h} symmetry) and Pyramidal (C_{3v}) symmetry) structures of compound NH_3 calculated at the HF/STO-3G level of theory, are given in Table 1.

Table 1: STO-3G calculated Zero-Point ZPE and Corrected Electronic Energies (E_o = Eel+ ZPE) for the Planar (D_{3h} Symmetry) and Pyramidal (C_{3v} Symmetry) Geometries of Compounds NH_3. Values are in Hartree except numbers in parenthesis that is in kcal mol^{-1}

Method	ZPE	E_o	ΔE_o	G	ΔG
Molecule		NH_3			
D_{3h}	0.037552	-55.400113	0.015182 (9.53)[a]	-55.417447	0.015923 (9.99)[a]
C_{3v}	0.040124	-55.415295	0.000000	-55.433370	0.000000
$C_{3v'}$	0.040124	-55.415295	0.000000	-55.433370	0.000000

The distortions of high-symmetry (D_{3h}) configuration of NH_3 molecule is due to the pseudo Jahn-Teller effect (PJTE). The main contributions to the distortions of high-symmetry (D_{3h}) configuration to its corresponding C_{3v} form of compound is mainly due to the PJTE by mixing

the ground A_1' and excited A_2'' state associated with mixing of $\psi_{HOMO}(a_2'')$ and ψ_{LUMO} (a_1') orbital in studied compound resulting in a PJT $[A_2''+ A_1']\otimes a_2''$ problem [13].

Transition state theory (TST) and Nitrogen inversion

Transition state theory assumes that the transition sate and reactants are in equilibrium and static mechanics info such as rate constants. Nitrogen inversion causes the interconversion of the both C_{3v} isomers of NH_3. K_{eq}=1 and the rate of inversion is so fast that they cannot be separated.

Kinetic studies Interconversions between pyramidal reactions at T=298 K is calculated using:

$$k_r = \mathrm{x}\frac{k_B T}{h} e^{-\Delta G_r^{\ddagger}/RT}$$

Where k_B and h are the Boltzmann's and Planck's constants, T is the absolute temperature, Reaction symmetry number x =1 is taken into consideration for the studied reactions according to the point groups of symmetries of the all stationary points [14-15]. So:

$$k_r = \frac{k_B T}{h} e^{-\Delta G_r^{\ddagger}/RT}$$

$\Delta G^{\ddagger}$ is the activation energy, defined as the difference between zero-point vibrational energies (ZPVE) of the transition state and the reactant. Δn_g the difference between the moles is the transition state and the initial state, because in inversion, the number of moles is equal in both cases, Therefore $k_{\text{inversion}}$ is equal with $k_{\text{rate constants}}$.

$$k_r = \frac{k_B T}{h} (RT)^{\Delta n_g} e^{-\Delta G_r^{\ddagger}/RT}$$

$$k_{-r} = \frac{k_B T}{h} (RT)^{\Delta n_g} e^{-\Delta G_{-r}^{\ddagger}/RT}$$

$$K_{eq} = \frac{k_r}{k_{-r}} = \frac{e^{-\Delta G_r^{\ddagger}/RT}}{e^{-\Delta G_{-r}^{\ddagger}/RT}} = 1$$

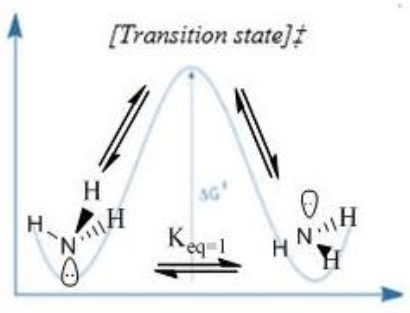

$\Delta G^{\ddagger}$: Change in Gibbs energy from reactants to TS

Figure1: Rate constants and Energy profile for the Interconversions between pyramidal reactions

The intrinsic reaction coordinate (IRC) [**16**] analysis has been carried out in both directions (forward and backward) along the reaction path in order to check the energy profiles connecting the identified transition structure to the associated energy minima [**17**]. In the present work,

transition state theory (TST) calculations have been performed in conjunction with a detailed exploration of the IRC path at the HF/STO-3G level of theory. 20 points and 5 steps on both the forward and reverse directions from the transition state position.

The resulting IRC calculations correspond to an optimization in the direction of the negative vibrational frequency of the transition state, i.e., a saddle point should have one imaginary frequency [**18**].

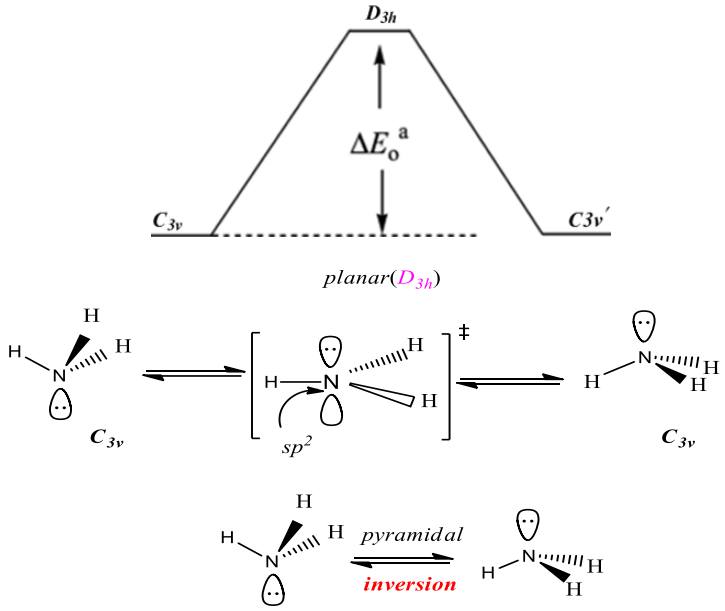

Figure2: Representation of interconversions between pyramidal [refs 19]

Structural parameters

The result indicates that bond distances are larger in C_{3v} symmetry in compared to D_{3h} symmetry. Also, it can be found ∠H-N-H bond angles are decreased with decreasing of symmetry (To see Figure2).

Table 2. Calculated Structural Parameters of the Planar (TS, D_{3h} Symmetry) and pyramidal (C3v Symmetry) Geometries of NH_3

Geometry NH_3	Bond lengths (Å) r N-H	Bond Angles(°) ∠HNHs	Torsion Angles(°)
D_{3h} (TS)	1.000	120˚.0	-----

C_{3v}	1.032	104˚.20	108.9764367

Molecular orbital analysis

Table 3. Lists the Structural parameters, frontier orbitals analysis (HOMO, LUMO), hardness, and chemical potential of NH_3 molecule.

NH_3	ε HOMO	ε LUMO	ε LUMO-ε HOMO	Δ chemical potential (μ)	Hardness(η)	$\Delta[\eta_{(C3v)}-\eta_{(D3h)}]$
TS, D_{3h}	-0.31153	0.59655	0.90808	0.14251	0.45404	0.000
C_{3v}	-0.35840	0.62496	0.98336	0.13328	0.49168	0.03776

On the other hand, in the effect of distortion of D_{3h} structure to C_{3v} structure decreases HOMO energy value with decreasing of the chemical potential. In contrast, LUMO energy value increases with increasing of hardness in the C_{3v} structure. Both parameters root-mean-square deviation (RMSD) and root mean square fluctuation (RMSF) define as a difference between two structures for a specific set of atoms and the Fluctuation around an average, respectively. The RMSF value is used to measure the flexibility of a structure (parameters of the system) and this value for the D_{3h} structure is less in comparison with the C_{3v} structure.

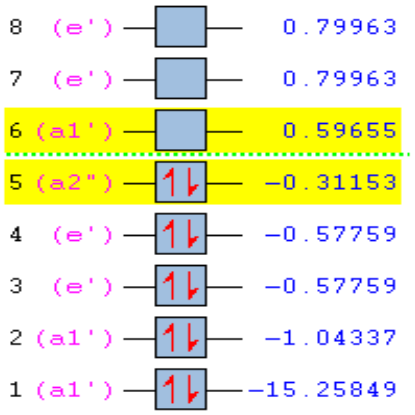

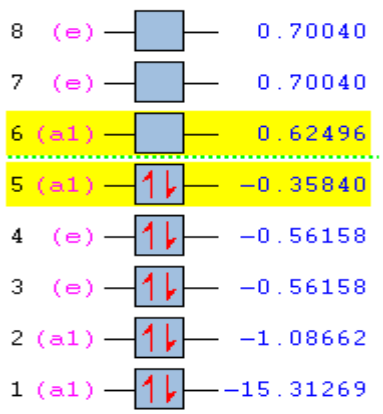

Distortion

Pyramid

$\Psi^*_0 \times \Psi_{1=} a''_2 \times a'_{1=} a''_2$

Orbital	Symmetry in D_{3h}		Symmetry in C_{3v}
HOMO	$1a''_2$	→	$3a_1$

LUMO	$3a'_1$	→	$4a_1$

Figuer3: Diagrams of HOMO and LUMO Orbitals in D_{3h} and C_{3v} structures of NH_3 molecule

The plot 3 revealed that $1a_2''$ (D_{3h}) MO becomes $3a_1$ (C_{3v}), and $3a_1'$ (D_{3h}) MO becomes $4a_1$ (C_{3v}) and these orbitals now have the same symmetry and can potentially mix.

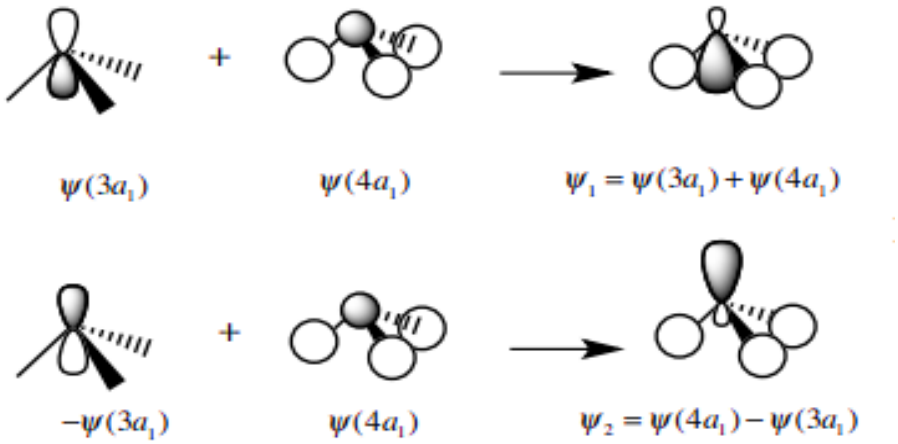

Figure4: Mixing of the $3a_1$ and $4a_1$ MOs for NH_3 [refs 20]

NH_3 has 8e (To see diagram 2) which fill this diagram to the $3a_1$ level. While the $3a_1$ MO is not stabilized by the geometry change, the loss of symmetry means that mixing can now occur between the occupied $3a_1$ and unoccupied $4a_1$ MO. This mixing is very strong and stabilizes the $3a_1$ MO substantially and hence NH_3 is trigonal pyramidal and not planar. The extent of mixing is determined by Rules for MO mixing: [1]only MOs of the same symmetry can mix [2] mixing must stabilize the total energy of the molecule [20].

Mixing tends to be large when at least one of the following criteria are met: MOs are close in energy, one of the MOs is non-bonding or unoccupied, MOs are in the HOMO-LUMO region

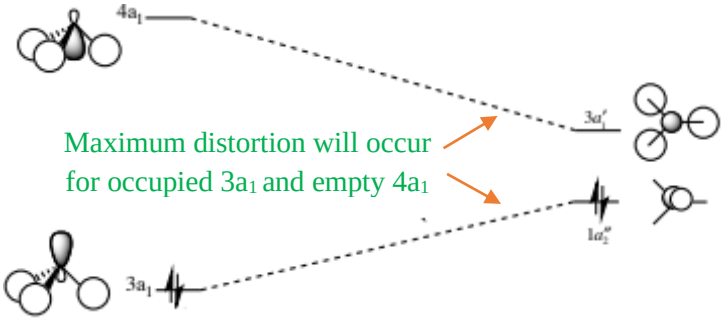

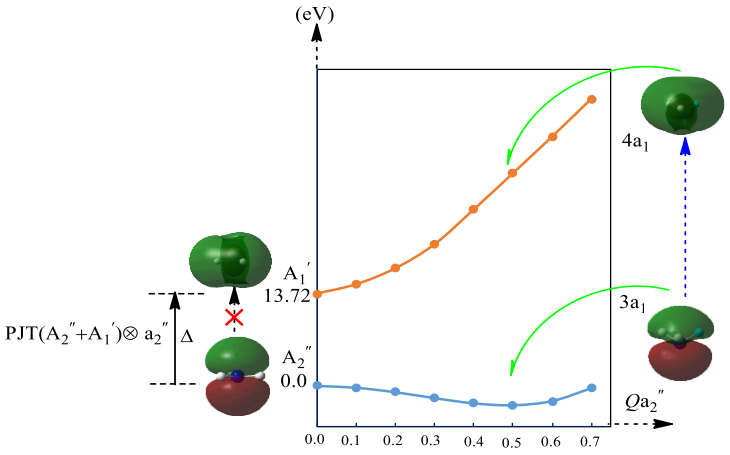

Figure5: Correlation diagram for mixing pyramidalization of $3a_1$ and $4a_1$ MOs [refs 20], and representation energies of the ground and excited state and its change along the distortion coordinate, respectively [Qa_2'']

It turns out that the strength of the Jahn-Teller effect is inversely proportional to the difference in energy between the two unmixed orbitals. The idea is that orbitals close in energy interact more strongly with each other - and that should be a somewhat familiar idea, because it is a central principle of MO theory. Anyway, it means that if the HOMO-LUMO gap in D_{3h} is *small*, which corresponds to a *smaller* energy barrier to planarization.

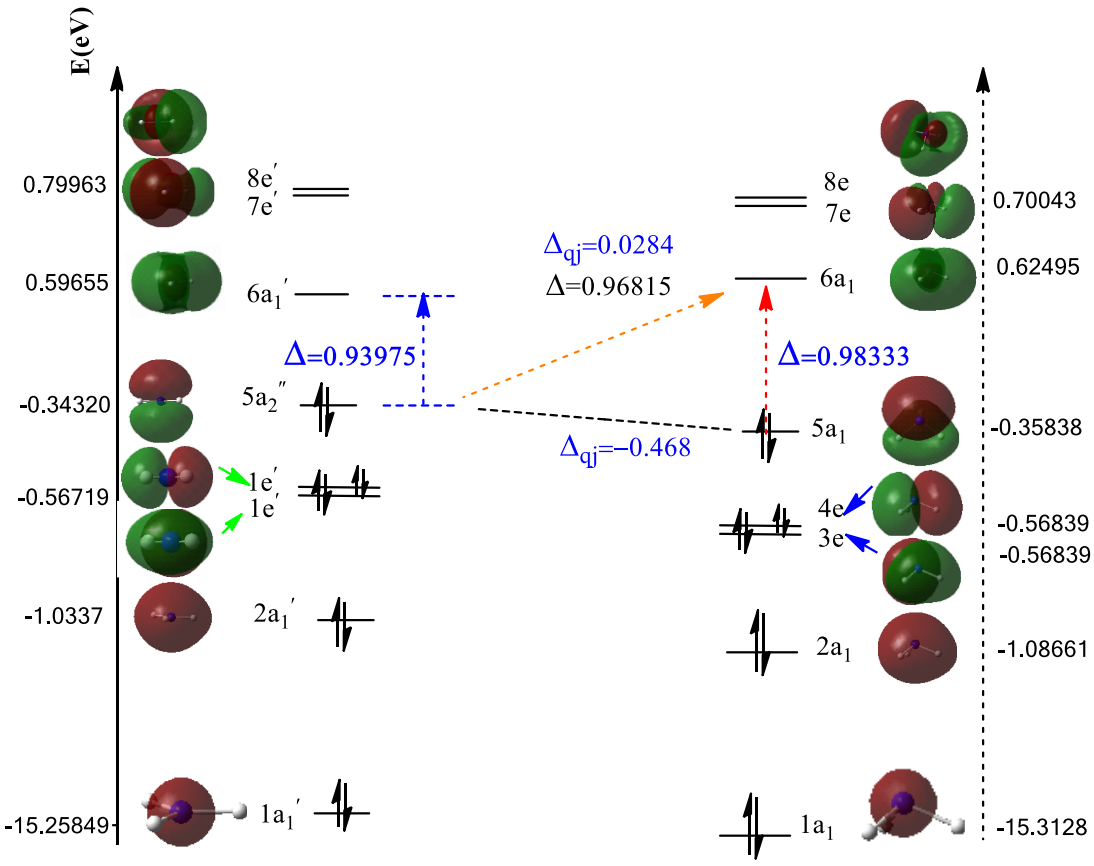

The present paper explores the orbital charge transfer (OCT) Δqi<<*ne* can be considered as a perturbation to the local n- electron subsystem. [21].The energy gap between orbitals is one of the parameters of controlling the transfer of pure charge in the interacting to the receiver.

Pauli Exchange-Type Repulsion (PETR)

In accordance with a well-established physical picture of steric repulsions, the steric exchange repulsion (as the energy difference due to orbital orthogonalization) can be estimated by means of the natural steric analysis [10]. The Pauli exchange type repulsion (or steric exchange energy) includes effects from all occupied orbitals and therefore typically contains contributions from covalent (intrabond) groups.

Table 4. shows the list of total steric exchange energy (TSEE) values in this compound , that obtained with natural atomic charge (*Q*(N) *and Q*(H)) values in the D_{3h} and C_{3v} structures of NH_3 molecule at the HF/STO-3G level of theory .

NH_3 structures	*Q*(N)	*Q*(H)	$Q = Q(N) - Q(H)$
D_{3h}	-0.53376	0.17792	-0.712
C_{3v}	-0.43500	0.14500	-0.580

This result demonstrates that the steric repulsions in the (C_{3v}) form increases with increasing of hardness and N—H Bond Lengths (Å) in the C_{3v} structure (see Table 1). Moreover, based on the obtained value, the more stable structure has greater total steric exchange energy (TSEE).

Natural Bond Analysis (NBO) analysis

The population analysis has also been performed by the natural bond orbital method at the HF/STO-3G level of theory on the optimized structure by using the NBO 6.0 program under Gaussian 2009 program [22-23].

Table 5. Calculated bonds occupancies by using natural bond analysis (NBO) by HF/STO-3G level method orbital Method HF/STO-3G level Occupancy

Method	**HF/STO-3G**		
	Occupancy		
Compound	NH_3 bent	Transition State	NH_3 bent′
BD (1) N 1 - H 2	1.99860	1.99666	1.99860
BD (1) N 1 - H 3	1.99860	1.99666	1.99860
BD (1) N 1 - H 4	1.99860	1.99666	1.99860
LP (1) N 1	2.00000	2.00000	2.00000

The stabilization energies associated with the electron delocalization have significant impacts on the energy differences between the different configurations of the molecules [15]; we conducted NBO analyses to estimate quantitatively the magnitude of the plausible donor- acceptor hyperconjugative interactions. It should be noted that the stabilization energies associated with BD (1) N - H $\rightarrow$ BD*(1) N - H electron delocalization's in the C_{3v} configuration of compound **is** more than the corresponding value for the BD (1) N- Hs $\rightarrow$ BD*(1) N- Hs electron delocalization in compared with D_{3h} configuration. The relative of formed N- H bonds with

can be illustrated as SP^2 and $Sp^{3.68}$ NH_3 structure with D_{3h}, and C_{3v} symmetries, respectively. The observed that with increasing p character of the σ – bonds C_{3v} symmetry of NH_3 molecule the occupancy increases, in contrast D_{3h} symmetry, which can explain the increase of the trans-bending and, consequently, the corresponding N-atom inversion process intrinsic distortion in the analysis of the Jahn-Teller effect. Deviations of N–Hs **σ-bonding** orbital by NBO analysis showed that there is no deviation in NH_3 molecule with D_{3h} symmetry, while in C_{3v} configuration the N–**Hs** σ-**bonding** deviate about 1.4°. The occupancy of the N–Hs **σ-bonding** orbital for C_{3v} configuration increases with descending of symmetry increased the stability of molecule.

As a shown in the output, this particular NBO, search terminated successfully after only a single, which satisfied the default search criteria. "cycle " The search yielded a Lewis structure with The search yielded a Lewis structure with one core (CR), three bond (D), and one lone pair (LP) for Lewis-type NBOs, which described about 99.900% of the total electron density(i.e. 9.98998 of the 10 electrons in planar) vs 99.958% % of the total electron density (i.e. 9.99579 of the 10 electrons in pyramidal). Moreover, the N hybrid to H ($sp^{3.68}$) is seen to be slightly rich in p-character (78.61%) in C_{3v} structure than the N hybrid to H ($sp^{2.00}$) in p-character (66.67%) in planar structure with D_{3h} symmetry. On other hand, output shown that LP_N is P-orbital pure ($p^{1.00)}$ in D_{3h}, while LPN is s (35.83%) p 1.79(64.17%) in C_{3v} structure.

The three λ_i values for the nitrogen NHOs:

N hybrids: $\lambda_{H1=}\ \lambda_{H2=}\lambda_{H3=}2.00$ (in D_3h)

$$\omega = cos^{-1}\left[-1/(2*2)^{1/2}\right]=120.0^{\circ}$$

N hybrids: $\lambda_{H1=}\ \lambda_{H2=}\lambda_{H3=}3.68$ (in C_3v)

$$\omega = cos^{-1}\left[-1/(3.7*3.7)^{1/2}\right]= 105.68^{\circ}$$

The result showed that the θ_{H-N-H} bonds angles for NH_3 in both planar and pyramidal structures are120.0°, 104.20°, respectively, while NBO analysis showed that the θ_{H-N-H} bond angles have rather small deviations (~1.4°) of the line of nucleus center in pyramidal structure, and the θ_{H-N-H} bond angles are 105.67°and it can be attributed to the bond strain. In other word, the optimized geometry exhibits slightly reduced H-N-H angles (104.20°), seemingly related with higher *s*-character in the n_N lone pair alongwith greater p-character in the σ_{N-H} hybrids.

NH_3: σ_{N-H} =0. 77($sp^{2.00}$+0.64 (s_H) , Nn=$p^{1.00}$ (planar, D_{3h})

NH_3: σ_{N-H} =0. 73($sp^{3.68}$+0.65 (s_H) , Nn=$sp^{1.79}$ (pyramidal, C_{3v})

Canonical molecular orbital (CMO)

The contributions of the corresponding molecular orbitals by means of the CMO method. In this approach, each molecular orbital can be expressed in terms of the complete orthonormal set of NBOs. Based on the CMO results, full quantitative details of the linear combinations of NBOs in terms of the complete orthonormal set of NBOs in the investigated compounds are given in Table 6. OF course, in this study, natural hybrid orbital calculations showed how the HOMO and LUMO orbitals were mixed. The results of these calculations did not match the data obtained from vibronic transitions.

The CMO analysis showed that ψ_{HOMO} (a_2'') and ψ_{LUMO} (a_1') belong to lone pair of the electrons (non-bonding pair of electrons) and σ*(N—H) of N atom, respectively.

ψ_{HOMO}= LP (1) N 1(lP)

ψ_{LUMO}=-0.576 (σ^*_{N1-H4}+σ^*_{N1-H3} + σ^*_{N1-H2})

Conclusions

The above reported theoretical studies provide a reasonable picture from intrinsic distortion in the analysis of the Jahn-Teller effect of [NH_3] molecule at the HF/STO-3G level of theory and showed:

1. The changing of bond length, bond angle and torsional angles (r, θ, Φ) play a crucial role in deformation a molecule. In this study, total Energy along IRC of [NH_3] molecule indicated that a decrease in the symmetry increased the stability of molecules. This increasing stability is attributed to PJTE. The vibronic coupling interaction between $^1A_2$" ground and the first $^1A_1'$ excited states via ($^1A_2$" + $^1A'_1$) ⊗ a_2" PJTE problem. The emergence of the pseudo Jahn-Teller effect of multi-atom systems in the form of a hybrid mixing of the basic electron and excited states is the only source of instability and spontaneous symmetry failure in the configuration of high symmetry structures in non-degenerate states. The Spontaneous symmetry breaking happens when one of the parameters (r,θ,ϕ) of the system reaches a critical value, so that the

system achieves the symmetry that has the least energy in applying that parameter. It is used as a general tool for better understanding the molecular structure and properties of systems

2. The principles of minimum energy (MEP), and maximum hardness (MHP) played a significant role in justifying the increased stability of the C_{3v} structure of NH_3 molecule.
3. The calculated natural atomic charge differences between the N and H atoms [*Q*(N)-*Q*(H)] in the C_{3v} structure increases with decreasing of chemical potential ***(μ).***
4. ∠H-N-H- bond angles are decreased with decreasing of symmetry.

5. The result showed that the θ_{H-N-H} bonds angles for NH_3 in both planar and pyramidal structures are120.0°, 104.20°, respectively, while NBO analysis showed that the θ_{H-N-H} bond angles have rather small deviations (~1.4°) of the line of nucleus center in pyramidal structure, and the θ_{H-N-H} bond angles are 105.67°and it can be attributed to the bond strain.

References

[1] L. Deng, T. Ziegler and L. Fan, *J. Chem. Phys.*, 99, 3823 (1993).

[2] C. Gonzalez, and H. B. Schlegel, *J. Phys. Chem.,* 94, 14, 5523 (1990).

[3] Gaussian 09, Revision C.01, Gaussian, Inc., Wallingford CT, 2009.

[4] I. I. R. Dennington, T. Keith, J. Millam, K. Eppinnett, W. L. Hovell, and R. Gilliland, GaussView, Version 3.09, Semichem, Inc.: Shawnee Mission, KS, 2003. 32950, 1992.

[5] A. Szabo and N. S. Ostlund. Modern Quantum Chemistry. Dover Publications, New York, 1989.

[6] I. N. Levine. Quantum Chemistry. Pearson Education (Singapore) Pte. Ltd., Indian Branch, 482 F. I. E. Patparganj, Delhi 110 092, India, 5th ed edition, 2003.

[7] K. Ohno; K. Esfarjani and Y. Kawazoe. Computational Material Science. Springer-Verlag, Berlin, 1999.

[8] E. Zahedi, S. Shaabani, and A. Shiroudi, *J. Phys. Chem. A.*, 121, 8504 (2017).

[9] G. Mahmoudzadeh, *Int. J. New. Chem.*, 6(4), 277 (2019).

[10] G. Mahmoudzadeh, R. Ghiasi, H. Pasdar, *J. Struct. Chem.*, 60, 736 (2019).

[11] AE. Reed, LA. Curtiss,F. Weinhold, *Chem. Rev.***,** 88, 899 (1988).

[12] ED. Glendening, JK. Badenhoop, AE. Reed, JE Carpenter, JA,Bohmann, CM. Morales, CR.Landis, F.Weinhold *NBO 6.0.* Theoretical Chemistry Institute, University of Wisconsin, Madison, WI,, 2013.

[13] D.Nori-Shargh, S. N. Mousavi, and J. E. Boggs, *J. Phys. Chem. A.*, 117, 7, 1621 (2013).

[14] M. D. Allendorf, T. M. Besmann, R. J. Kee, and M. T. Swihart, Chemical Vapor. Deposition: Precursors, Processes and Applications, 1st edn., The Royal Society of Chemistry, UK, 2009.

[15] K. A. Holbrook, M. J. Pilling, and S. H. Robertson, Unimolecular Reactions, 2nd edn. Wiley, Chichester, 1996.

[16] F. Fukui, *J. Phys. Chem.*, 74, 4161 (1970).

[17] A. R. Oliaey, A. Shiroudi, E. Zahedi, and M. S. Deleuze, *React. Kinet. Mech. Cat.*, 124, 27 (2018).

[18] Z.Kazminejad, A. Shiroudi, and et.al, *J. Chil. Chem. Soc.*, 64, 1 (2019).

[19] j. D. Robert, and M. C. Caserio (1977) *Basic Principles of Organic Chemistry, second edition.* W. A. Benjamin, Inc., Menlo Park, CA. ISBN 0-8053-8329-8.

[20] http://www.huntresearchgroup.org.uk/teaching/year1_lab_start.html

[21] I. Balan, I. Arsene, and N.N. Gorinchoy, 20 international symposium on the jahn teller, (2010).

[22] A. E. Reed, R. B. Weinstock, and F. Weinhold, *J. Chem. Phys.*, 83, 735 (1985).

[23] J. K. Badenhoop, and F. Weinhold, *Int. J. Quantum. Chem.*, 72, 269 (1999).

How to Cite This Article

Golrokh Mahmoudzadeh, **"Intrinsic distortion in the analysis of the Jahn-Teller effect: by Transition state theory (TST) and Nitrogen inversion"** International Journal of New Chemistry., 2021; DOI: 10.22034/ijnc.2020.138177.1133.